HHS Public Access

Author manuscript

Addiction. Author manuscript; available in PMC 2024 February 16.

Published in final edited form as:

Addiction. 2024 January ; 119(1): 113–124. doi:10.1111/add.16330.

Brain structural covariance network features are robust markers of early heavy alcohol use

Jonatan Ottino-González[1,2], **Renata B. Cupertino**[3], **Zhipeng Cao**[2], **Sage Hahn**[2], **Devarshi Pancholi**[2], **Matthew D. Albaugh**[2], **Ty Brumback**[4], **Fiona C. Baker**[5], **Sandra A. Brown**[6], **Duncan B. Clark**[7], **Massimiliano de Zambotti**[5], **David B. Goldston**[8], **Beatriz Luna**[7], **Bonnie J. Nagel**[9], **Kate B. Nooner**[10], **Kilian M. Pohl**[5,11], **Susan F. Tapert**[12], **Wesley K. Thompson**[13], **Terry L. Jernigan**[14], **Patricia Conrod**[15], **Scott Mackey**[2], **Hugh Garavan**[2]

[1]Division of Endocrinology, The Saban Research Institute, Children's Hospital Los Angeles, Los Angeles, CA, USA

[2]Department of Psychiatry, University of Vermont Larner College of Medicine, Burlington, VT, USA

[3]Department of Genetics, University of California San Diego, San Diego, CA, USA

[4]Department of Psychological Science, Northern Kentucky University, Highland Heights, KY, USA

[5]Center for Health Sciences, SRI International, Menlo Park, CA, USA

[6]Departments of Psychology and Psychiatry, University of California, San Diego, La Jolla, CA, USA

[7]Department of Psychiatry, University of Pittsburgh, Pittsburgh, PA, USA

Correspondence: Jonatan Ottino-González, Division of Endocrinology, The Saban Research Institute, Children's Hospital Los Angeles, Los Angeles, CA, USA. jongonzalez@chla.usc.edu.

AUTHOR CONTRIBUTIONS

Jonatan Ottino-González: Conceptualization (lead); data curation (lead); formal analysis (lead); methodology (lead); visualization (lead); writing—original draft (lead). **Renata B. Cupertino:** Conceptualization (supporting); writing—review and editing (supporting). **Zhipeng Cao:** Conceptualization (supporting); writing—review and editing (supporting). **Sage Hahn:** Conceptualization (supporting); resources (supporting); writing—review and editing (supporting). **Devarshi Pancholi:** Data curation (supporting); resources (supporting); software (supporting); writing—review and editing (supporting). **Matthew D. Albaugh:** Conceptualization (supporting); supervision (supporting); writing—review and editing (supporting). **Ty Brumback:** Resources (supporting); writing—review and editing (supporting). **Fiona C. Baker:** Resources (supporting); writing—review and editing (supporting). **Sandra A. Brown:** Resources (supporting); writing—review and editing (supporting). **Duncan B. Clark:** Resources (supporting); writing—review and editing (supporting). **Massimiliano de Zambotti:** Resources (supporting); writing—review and editing (supporting). **David B. Goldston:** Resources (supporting); writing—review and editing (supporting). **Beatriz Luna:** Resources (supporting); writing—review and editing (supporting). **Bonnie J. Nagel:** Resources (supporting); writing—review and editing (supporting). **Kate B. Nooner:** Resources (supporting); writing—review and editing (supporting). **Kilian M. Pohl:** Resources (supporting); writing—review and editing (supporting). **Susan F. Tapert:** Resources (lead); writing—review and editing (supporting). **Wes K. Thompson:** Resources (supporting); writing—review and editing (supporting). **Terry L. Jernigan:** Resources (lead); writing—review and editing (supporting). **Patricia Conrod:** Funding acquisition (lead); resources (lead); writing—review and editing (supporting). **Scott Mackey:** Conceptualization (supporting); funding acquisition (lead); project administration (lead); supervision (lead); writing—review and editing (supporting). **Hugh Garavan:** Conceptualization (supporting); funding acquisition (lead); project administration (lead); supervision (lead); writing—review and editing (supporting).

SUPPORTING INFORMATION

Additional supporting information can be found online in the Supporting Information section at the end of this article.

[8]Department of Psychiatry and Behavioral Sciences, Duke University School of Medicine, Durham, NC, USA

[9]Departments of Psychiatry and Behavioral Neuroscience, Oregon Health and Science University, Portland, OR, USA

[10]Department of Psychology, University of North Carolina Wilmington, Wilmington, NC, USA

[11]Department of Psychiatry and Behavioral Sciences, Stanford University, Stanford, CA, USA

[12]Department of Psychiatry, University of California San Diego, San Diego, CA, USA

[13]Department of Radiology, University of California San Diego, San Diego, CA, USA

[14]Center for Human Development, University of California, San Diego, CA, USA

[15]Department of Psychiatry, Université de Montreal, CHU Ste Justine Hospital, Montreal, Québec, Canada

Abstract

Background and Aims: Recently, we demonstrated that a distinct pattern of structural covariance networks (SCN) from magnetic resonance imaging (MRI)-derived measurements of brain cortical thickness characterized young adults with alcohol use disorder (AUD) and predicted current and future problematic drinking in adolescents relative to controls. Here, we establish the robustness and value of SCN for identifying heavy alcohol users in three additional independent studies.

Design and Setting: Cross-sectional and longitudinal studies using data from the Pediatric Imaging, Neurocognition and Genetics (PING) study (n = 400, age range = 14–22 years), the National Consortium on Alcohol and Neurodevelopment in Adolescence (NCANDA) (n = 272, age range = 17–22 years) and the Human Connectome Project (HCP) (n = 375, age range = 22–37 years).

Cases: Cases were defined based on heavy alcohol use patterns or former alcohol use disorder (AUD) diagnoses: 50, 68 and 61 cases were identified. Controls had none or low alcohol use or absence of AUD: 350, 204 and 314 controls were selected.

Measurements: Graph theory metrics of segregation and integration were used to summarize SCN.

Findings: Mirroring our prior findings, and across the three data sets, cases had a lower clustering coefficient [area under the curve (AUC) = −0.029, P = 0.002], lower modularity (AUC = −0.14, P = 0.004), lower average shortest path length (AUC = −0.078, P = 0.017) and higher global efficiency (AUC = 0.007, P = 0.010). Local efficiency differences were marginal (AUC = −0.017, P = 0.052). That is, cases exhibited lower network segregation and higher integration, suggesting that adjacent nodes (i.e. brain regions) were less similar in thickness whereas spatially distant nodes were more similar.

Conclusion: Structural covariance network (SCN) differences in the brain appear to constitute an early marker of heavy alcohol use in three new data sets and, more generally, demonstrate the utility of SCN-derived metrics to detect brain-related psychopathology.

Keywords

Alcohol; cortical thickness; early marker; graph theory; neurodevelopment; structural covariance networks

INTRODUCTION

Alcohol use produces substantial health costs, is a leading cause of preventable mortality world-wide [1] and a significant proportion of alcohol users go on to develop an alcohol use disorder (AUD) [2]. In adults, alcohol use has been linked to lower gray matter volume relative to controls [3–6] in widespread parts of the brain and, in adolescents, is related to a typical neurodevelopment [7–10]. Brain differences have also been reported in alcohol-naïve individuals with a family history of AUD [11]. However, these brain findings have been highly heterogeneous and challenging to reproduce with conventional mass-univariate tests [12]. Multivariate approaches may provide a better characterization of the complex interaction of the brain with alcohol use and AUD.

Recently, we reported differences in structural covariance networks (SCN) assessed with graph theory metrics in young adults with AUD and adolescents with present and future problematic alcohol use [13]. SCN represents the correlation of cortical thicknesses between different brain regions. The biological basis of SCN involves multiple factors including underlying patterns of cortico–cortical growth. Covarying regions possibly share common plastic and trophic influences on cortical thickness as they proceed through the same developmental stages or are impacted similarly by external stimuli [14]. Graph theory metrics summarize SCN patterns by mapping all pairwise correlations among brain regions as a network and extracting global features [15]. Correlations above a threshold, termed ‘edges’, reveal how coordinated in thickness two regions, or ‘nodes’, are. Consequently, the relationships between nodes reveal the degree of cortico–cortical similarity.

Our prior work utilized two of the largest sources of magnetic resonance imaging (MRI) data with alcohol use phenotyping: the pooled ENIGMA-Addiction data sets (n = 1495, https://www.enigmaaddictionconsortium.com) and the IMAGEN study of adolescent development (n = 891, https://imagen-project.org). We found that a distinct pattern of SCN, namely lower segregation and higher integration, characterized young adults with AUD (n = 745) and adolescents with hazardous drinking at age 19 (n = 297) and at age 14 prior to substantial use, indicating that SCN differences may be a risk factor for problematic use. Our results suggested that the alcohol using adults and at-risk youth showed a pattern where, compared to controls, distant brain regions were more similar in thickness while brain regions closer to each other were less similar in thickness. A similar network profile (i.e. lower segregation and higher integration) has been found in other substance and non-substance use disorders using resting-state and diffusion MRI [16–20]. It has been hypothesized that imbalances in segregation and integration may reflect differences in neurodevelopmental trajectories [21] related to lower executive functions and greater internalizing symptoms [22–27] which could contribute to early alcohol onset and ongoing problematic use. The present study had therefore three aims:

1. To demonstrate the robustness and value of SCN to identify individuals with heavy alcohol use by replicating our prior findings on three new independent data sets.
2. To investigate whether multivariate methods, namely the analysis of SCN, and univariate methods, such as single region-of-interest (ROI) contrasts, produce similar outcomes.
3. To locate which nodes are showing lower segregation in cases compared to controls and to provide insights on the relationship between segregation and integration.

MATERIALS AND METHODS

Participants

Procedures were approved by institutional review at each site and all participants provided informed consent. All data sets were treated cross-sectionally.

Pediatric Imaging, Neurocognition and Genetics (PING)

The PING study collected behavioral and MRI data on 1493 individuals aged 3–20 years at 10 sites [28]. Cases endorsed one or more problems with alcohol use (e.g. health or psychological sequelae, reckless behavior, tolerance/withdrawal). See Supporting information for the full set of criteria (Supporting information, S1); 50 cases and 350 age- and sex-matched controls were identified ($n = 400$).

National Consortium on Alcohol and Neurodevelopment in Adolescence (NCANDA)

NCANDA is an ongoing accelerated longitudinal study of early alcohol use, including annual assessments of 831 individuals recruited between the ages of 12 to 21 years at five sites [29]. To match the age range (17–22 years) in our previous work, analyses were based on participants between the ages 17 to 22. Participants meeting the age range criteria were only included once (i.e. 302 from baseline, 242 from year 3 and 164 from year 5). Groups were formed using published NCANDA criteria [8, 10, 30–34] for heavy alcohol use. Briefly, those that surpassed age-dependent life-time drinking days thresholds (e.g. > 23 at age 17 years, > 51 for +18 years), were in the 75th quartile of life-time binge drinking episodes and were heavy drinkers after Calahan's criteria were considered cases. Controls did not surpass life-time drinking days thresholds, had no life-time binge drinking episodes and were not heavy drinkers; 68 cases and 204 matched controls were identified (see Supporting information, S2 for details) ($n = 272$).

Human Connectome Project (HCP)—S1200 release

HCP is a large publicly available imaging data set [35]. We used the S1200 release, which includes data on 1113 participants aged 22–36 years. Cases were selected based on DSM-IV-TR criteria for life-time alcohol dependence. Controls did not endorse any life-time symptoms; 61 cases and 314 controls, all unrelated, were identified (see Supporting information, S3 for details) ($n = 375$).

Imaging

We used the average cortical thicknesses of ROIs derived from Desikan atlas in FreeSurfer [36, 37]. The insula ROI label was not included in version 4.1 used to prepare the PING data set. NCANDA and HCP data were prepared with versions 5.1 and 5.3, respectively, which include the insula ROI. Hence, 66 bilateral ROIs were analyzed for PING and 68 ROIs for NCANDA and HCP. Details on the MRI protocols and processing pipelines of each study are published elsewhere [9, 28, 38]. Scanner effects in PING (12 scanners) and NCANDA (five scanners) were adjusted for each ROI with *ComBat* version 1.0.13 [39] while preserving age, sex and group effects as in our prior work. HCP data were collected on a single MRI scanner.

SCN construction and graph theory metrics

The generation of SCN and the extraction of graph theory metrics were performed separately for each data set. Prior to the SCN construction, each scanner-adjusted ROI was residualized for mean global thickness. For cases and controls independently, SCN were generated by calculating the Pearson's correlation between every pair of residualized ROIs. The correlation coefficients of each group were binarized according to a series of thresholds following a density-based approach to ensure SCN were equal in size (i.e. groups were matched for the number of edges) [40]. Thresholds increased in 1% increments starting at the minimum density (D_{min}), where groups showed fully connected graphs up to a density preserving the top 30% of the edges.

Graph theory metrics summarize SCN organization at several levels of complexity: edge (e.g. correlation coefficients), node (e.g. transitivity) and network (e.g. modularity). Network metrics of segregation and integration were calculated for each group and density (Figure 1). Briefly, greater segregation [i.e. higher clustering coefficient (Cp), local efficiency (LE) or modularity] indicates greater correspondence among adjacent nodes and greater integration [i.e. lower average shortest path length (Lp) or greater global efficiency (GE)] indicates higher correspondence among distant nodes. See Supporting information for more information.

We formerly reported a pattern of lower SCN segregation (lower Cp, LE and modularity) and higher integration (lower Lp and higher GE) in individuals with heavy alcohol use [13] suggesting fewer short-range edges and more long-distant edges. To explore whether these phenomena were related, node-level metrics of transitivity, participation coefficient (PC) and within-modular degree (WMD) were calculated. Transitivity is a segregation metric reflecting the number of closed triangles per node (i.e. whether neighbors of a node are neighbors of each other). As nodes that are similar in thickness should be assorted to the same module, PC and WMD could clarify why some nodes are poorly segregated. PC captures how similar in thickness a node is to nodes from other modules, where higher values of PC represent more intermodular, long-distance edges [41]. Conversely, WMD captures how similar in thickness a node is to other nodes in its own module, i.e. the number of intramodular, short-range edges [41]. Consequently, PC and WMD shed light upon whether a node with low segregation (low transitivity) is caused by more intermodular edges (high PC), fewer intramodular edges (low WMD) or both. See Supporting information, S5

for more details. A visual summary of the graph theory metrics used here is depicted in Figure 1. All steps were performed in *brainGraph* version 2.7.3 [42].

Statistical analysis

For each data set, differences in age and sex were assessed with *t*- and χ^2 tests. In PING and NCANDA, controls were matched to cases for age and sex with the *MatchIt* package version 3.0.2 [43] at the highest ratio possible where group differences were not found.

Mean and regional cortical thickness differences between cases and controls were examined with linear models. All *P*-values from the regional thickness contrasts ($n = 68$ in NCANDA and HCP, 66 in PING) were adjusted using false discovery rate (FDR, q-value < 0.05) [44]. All analyses were performed in R version 4.1.0 [45]. While aim 1 analysis sought to replicate our prior findings following the same analytical plan [13], aims 2 and 3 analyses were not pre-registered and results should be considered exploratory.

Aim 1—SCN replication of network-level contrasts

Prior to the SCN analysis, we examined a potential confound related to group differences in global correlation strength. If differences in the global correlation strength exist, spurious edges may be introduced by matching the groups in terms of SCN density. The confound was assessed with permutation-based *t*-tests (1000 iterations).

For the network-level contrasts, and similar to our previous work, a null distribution for statistical testing was generated with permutation tests (1000 iterations) for each density and SCN metric. Critical values from this null distribution were used to test the significance of the observed differences. To prevent results from relying on an arbitrary density, significance was defined as $P < 0.05$ for the area under the curve (AUC) across the range of tested densities. Lower Cp, LE, modularity and Lp, and higher GE in cases relative to controls, were expected based on our previous results.

To facilitate the interpretation of the results, and reduce the number of tests, further analyses explored the relationship between SCN-derived metrics and cortical thickness and located SCN effects at the node-level (Aim 2) and examined the interplay of segregation and integration (Aim 3) on the three pooled data sets after adjusting for study effects with ComBat [39]. That is, cortical thickness was first adjusted for scanner effects within study for the preceding analyses, and here additionally harmonized between studies. These pooled analysis were conducted using 66 ROIs.

Aim 2—Multivariate and univariate correspondence

First, to examine whether SCN-derived metrics were capturing additional information compared to cortical thickness alone, we generated a regional strength score that captures the average of all the correlation weights per ROI ($n = 65$) and conducted Spearman's correlation (rho) between these scores and the cortical thickness of each region ($n = 66$). Secondly, to explore if group regional differences in cortical thickness (*t*-values) were related to group differences in regional strength we (a) ran all possible Fisher's *Z*-tests to compare cases and controls on each pairwise correlation in the correlation matrix (66

× 65 = 4290/2 = 2145 tests), (b) averaged the resulting statistics for each one of the 66 ROIs (i.e. each ROI's average was based on its 65 Fisher's *Z*-test scores) and (c) calculated a Spearman's correlation between these average scores and the initial cortical thickness between-group *t*-values. As these scores are probably co-dependent because of anatomical proximity, *P*-values were adjusted (*P*-spin) for auto-spatial correlations as in Alexander-Bloch *et al.* [46] (see https://github.com/frantisekvasa/rotate_parcellation for details).

Aim 3—Segregation versus integration

Node-level comparisons were conducted in a similar manner as the network-level contrasts (Aim 1). We anticipated lower transitivity in cases. Nodes showing lower transitivity were tested for higher PC and lower WMD. Correlations (rho) among the unthresholded differences in transitivity, PC and WMD were tested to assess if lower transitivity was related (*P*-spin < 0.05) to a greater presence of intermodular edges (higher PC) or to a lesser number of intramodular edges (lower WMD).

RESULTS

Demographics

After the matching procedure, age and sex did not differ among cases and controls in the separate or pooled data sets. Table 1 summarizes the participant demographics.

Mean and regional cortical thickness differences

In PING and NCANDA, cases exhibited thinner mean cortical thickness than controls (PING: $t = 2.80$, $P = 0.005$; NCANDA: $t = 2.19$, $P = 0.030$). No regional cortical thickness differences were found after FDR correction. In HCP, there was no difference in mean cortical thickness ($t = 0.78$, $P = 0.436$) and no regional cortical thickness differences after FDR correction. Further, maps of regional cortical thickness differences (Figure 2b) were unrelated among data sets: PING-to-NCANDA rho = −0.08, $P = 0.51$; PING-to-HCP rho = 0.05, $P = 0.67$; NCANDA-to-HCP rho = 0.14, $P = 0.27$. In the pooled analysis, cases had lower mean cortical thickness compared to controls ($t = 3.23$, $P = 0.001$), and lower thickness in several regions survived FDR correction (Figure 2 and Supporting information, S6, S7, S8 and S9).

Aim 1—SCN replication of network-level contrasts

No group differences were found in the global correlation strength in PING ($t = -0.12$, $P = 0.90$), NCANDA ($t = -0.28$, $P = 0.78$), HCP ($t = 0.46$, $P = 0.66$) or in the pooled data sets ($t = -0.05$, $P = 0.96$). Figure 3a illustrates the distribution of the global correlation strength as well as group differences on this metric.

PING cases exhibited lower Cp ($P = 0.029$), lower modularity ($P = 0.039$), lower Lp ($P = 0.033$) and greater GE ($P = 0.023$) compared to controls. LE differences were not significant ($P = 0.112$). In NCANDA, cases exhibited lower Cp ($P = 0.028$), lower modularity ($P = 0.031$), lower Lp ($P = 0.012$) and higher GE ($P = 0.025$) relative to controls. Groups did not differ for LE ($P = 0.158$). With regard to HCP, cases had lower Cp ($P = 0.030$), lower Lp ($P = 0.014$) and higher GE ($P = 0.016$). Modularity ($P = 0.123$) and LE ($P =$

0.106) differences were not significant. In the pooled data sets, cases had lower Cp (P = 0.002), lower modularity (P = 0.004), lower Lp (P = 0.017) and higher GE (P = 0.010). LE differences were marginal (P = 0.052) (Figure 3c). Supporting information, S10 lists the full set of findings and results of a random-effects meta-analysis conducted on both the three data sets in the present work and the data sets in our prior paper (i.e. PING, NCANDA, HCP, ENIGMA-Addiction, IMAGEN baseline, IMAGEN follow-up). Additional analysis on sex differences were in the same direction as originally reported, although not all effects were significant, which was probably due to the lower number of participants (see Supporting information, S12). Supplementary tests on age and sex-adjusted SCN did not change the direction of the original results (see Supporting information, S12).

Aim 2—Multivariate and univariate correspondence

The relationship between regional strength and regional cortical thickness was non-significant and negative in both cases (rho = −0.34, rho^2 = 0.12, P-spin = 0.163) and controls (rho = −0.43, rho^2 = 0.18, P-spin = 0.063). Similarly, the relationship between the differences in regional correlation strength (i.e. average Fisher's Z-test scores per ROI) and regional cortical thickness (i.e. t-values) as non-significant and negative (rho = −0.25, rho^2 = 0.06, P-spin = 0.081).

Aim 3—Segregation versus integration

Cases had lower transitivity in several nodes (Supporting information, S11). Among the nodes with lower transitivity, cases presented greater PC in the left inferior parietal [AUC = 0.022, $95\%_{high}$ confidence interval (CI) = 0.016 P = 0.018], the left superior parietal (AUC = 0.013, $95\%_{high}$ CI = 0.012, P = 0.043), the left paracentral (AUC = 0.047, $95\%_{high}$ CI = 0.045 P = 0.035) and the right inferior parietal (AUC = 0.016, $95\%_{high}$ CI = 0.012 P = 0.021). No nodes lower in transitivity showed lower WMD. In addition, while the differences in transitivity and PC were negatively and significantly correlated (rho = −0.47, P-spin < 0.001), the differences in transitivity and WMD were not (rho = −0.02, P-spin = 0.479) (Figure 4b).

DISCUSSION

We replicated in three new independent data sets a SCN pattern that distinguishes heavy alcohol users from controls. As in our prior work [13], heavy alcohol users here showed lower segregation and higher integration, suggesting that adjacent cortical regions were less similar in thickness while spatially distant regions were more similar. The present analyses also yielded insights into the location and nature of the group differences in such pattern: lower segregation in cases (1) was mainly observed in frontal and parietal regions and (2) was related to a greater number of intermodular edges rather than fewer intramodular edges. In summary, this SCN pattern suggests that heavy alcohol use may be related to differences in normative cortico–cortical maturation.

AUD has previously been linked to gray matter differences in prefrontal and reward-processing areas [4, 5]; even low levels of alcohol use have been associated with premature brain aging [3, 47] and, in adolescents, alcohol use has been associated with accelerated

cortical thinning [8, 48]. Our results align with these prior findings—in all three data sets, cases exhibited thinner cortex than controls. However, none of the ROIs tested in each data set separately survived FDR correction. More importantly, the maps of regional cortical thickness differences were unrelated among data sets consistent with heterogeneity of findings resulting from univariate analyses.

In contrast to the heterogeneous results from mass-univariate tests on cortical thickness, the SCN global pattern consistently shows, among five independent data sets [13], that heavy alcohol use is related to lower cortical thickness correspondence among adjacent regions and higher similarity between distant regions. Similar SCN profiles have been reported with different MRI modalities in youth at-risk for AUD [16], adults with AUD [18] and other addictions [16, 18, 19]. Imbalances in segregation and integration have also been related to psychiatric and neurological disorders [48]. Two hypotheses emerge considering our findings. Alcohol neurotoxic effects [49, 50] might have precipitated subtle changes in anatomically distant nodes, resulting in increased correlations in thickness. An alternative is that SCN differences including the greater number of intermodular edges reflects developmental delays in regional specialization of functions [21]. Delayed neurodevelopment has been related to inattention and poor decision-making, self-regulation failures, greater reward-seeking behaviors and greater internalizing symptoms, all risk factors for early alcohol onset [22–27]. Although the cross-sectional nature of the data limits our ability to determine temporal order, our prior study [13] found the same SCN pattern, albeit not significant, in a smaller subsample of adolescents at age 14 who were alcohol-naïve, implying that subtle SCN differences may predate alcohol exposure.

Regarding the equivalence among multivariate and univariate approaches to cortical thickness data, we found that the correlations between the regional average correlation strength and the regional cortical thickness were weak, negative and non-significant in cases and controls. The correlation between-group differences for regional correlation strength and regional cortical thickness was also weak, negative and non-significant. These results suggest that multivariate and univariate estimates of brain structure provide distinct insights. Here we have demonstrated that the SCN results, derived from a multivariate method, were consistent throughout studies relative to mass-univariate tests results. This indicates that there is value in multivariate methods to study brain structure, and other studies might find this and other similar approaches useful.

Node-level metrics such as transitivity helped in localizing lower segregation effects in the brain. Consistent with patterns of lower Cp in cases, lower transitivity was observed broadly but especially in parietal and frontal nodes. Similarly, PC and WMD metrics clarified that lower segregation/transitivity was in part related to a greater number of edges with nodes from other modules. Relative to controls, four parietal nodes low in transitivity showed higher PC in cases. None of the nodes with low transitivity had lower WMD. Also, the maps of unthresholded group differences in transitivity and PC were negatively related: the lower the transitivity in cases, the greater the PC in this group. There was no relation between transitivity and WMD differences. In brief, some nodes appear to show less discrepancy from distant nodes and could be related to alterations in typical patterns of maturation-related differentiation, as we hypothesized [21, 51]. The lower modularity in cases supports

this conclusion. As Figure 4 shows, cases present aberrant modularity patterns (e.g. temporal nodes included in prefrontal modules). Modularity peaks by late adolescence [52, 53] and is related to the achievement of executive functions [54], cognitive skills that, when deficient, may contribute to early alcohol exposure [55, 56]. Other converging evidence also suggest brain maturation differences with heavy or binge alcohol use in human adolescents [8, 30, 34] and non-human primates [57]. In our study, the use of cross-sectional data prevents us from stating that SCN effects mimic other longitudinal works showing delays in brain growth. Longitudinal studies with sufficient data throughout the life-span will be able to confirm this.

Also critical to this work is what clinical value a brain marker identified at the group-level has. We have shown that early heavy alcohol use is related to deviations on patterns of thickness similarity among adjacent and distant regions, and that such deviations are observed in parietal and frontal regions [58, 59]. These regions experience intense remodeling during puberty and adolescence, developmental periods highly represented in this work. It is possible that early interventions help redirect cortico–cortical growth back to normative trajectories and lower the risk of alcohol use, yet the current work leaves unclear if effects precede or arise from use. Also, existing methods to generate individual-level measures on thickness covariance are the next step to offer better predictions. However, said methods are in part different and likely to yield distinct results from the ones we tried to replicate here [58–61]. It would nonetheless be valuable to examine whether other approaches also generate their own robust pattern of results across independent data sets.

The current work has several limitations. First, the criteria to define the problematic drinking groups varied between data sets, ranging from the heavy alcohol use in PING and NCANDA to clinical diagnosis of AUD in HCP. However, the observation of the same pattern of altered SCN among the different sets of criteria indicates that the phenomenon is robust and not simply an artifact of a specific definition of problematic use. Institutional restrictions on data sharing obstructed our ability to use the same FreeSurfer version, test alternative parcellations of the brain or run quality checks on the data. The consistency of findings despite differences in the preparation of the data also supports the apparent robustness of the pattern of results. In a similar vein, the optimal adjustment for scanner effects in multi-site collaborations is an ongoing topic of discussion [62], with new approaches inspired by the original ComBat process such as ComBat-GAM [63], CovBat [64] or LongCombat [65]. While we used the original ComBat to replicate our already published findings [13], other options could be explored in future work. Another limitation was the lack of control over the concomitant use of other drugs besides alcohol, onset of AUD, anxiety and depression symptoms, socio-economic status and education. While the cross-sectional nature of the data as used here cannot address whether the observed pattern of altered SCN precedes alcohol exposure, this may be examined in future studies with longitudinal adolescent samples.

In conclusion, the present study demonstrates that differences in structural covariance networks based on cortical thickness are sensible and robust markers of heavy alcohol use. In five independent studies, including three in this paper, individuals with heavy alcohol use showed SCN patterns of lower segregation and higher integration compared to controls suggesting that, in heavy alcohol users, adjacent regions of the brain were less similar in

thickness while spatially distant regions were more similar. This pattern of altered cortico–cortical correspondence was explained in part by a greater presence of intermodular edges, implying that deficits in the brain's modular organization are potentially related to delayed brain maturation.

Supplementary Material

Refer to Web version on PubMed Central for supplementary material.

ACKNOWLEDGEMENTS

The authors gratefully acknowledge the financial support that was instrumental in conducting this research and was provided by the National Institute on Alcohol Abuse and Alcoholism, the National Institute on Drug Abuse, the National Institute of Mental Health, the National Institute of Child Health and Human Development, (grants: U24 AA021697, U01 AA021696, U24 AA021695, U01 AA021692, U01 AA021691, U01 AA021690, U01 AA021681, and U01 AA02169) and the 2022 HAI-Google Cloud Credits Award. We also extend our sincere appreciation to the participants who generously volunteered their time for this study.

DECLARATION OF INTERESTS

M.d.Z. has received research funding unrelated to this work from Noctrix Health, Inc., Verily Life Sciences LLC. M.d.Z. is a co-founder of Lisa Health Inc., and has ownership of shares in Lisa Health. There are no further conflicts of interest to state by the rest of the authors.

DATA AVAILABILITY STATEMENT

Please direct data inquiries to Susan F. Tapert, PhD (NCANDA study, http://www.ncanda.org), Terry L. Jernigan, PhD (PING study, https://chd.ucsd.edu/research/ping-study.html) and the Human Connectome Project website (https://www.humanconnectome.org). NCANDA data were collected from 13 January 2013 to 15 January 2019 and were based on the formal locked data releases NCANDA_PUBLIC_4Y_REDCAP_V02* [64] and NCANDA_PUBLIC_4Y_STRUCTURAL_V01 [65]. Data were distributed to the public according to the NCANDA Data Distribution agreement; available at: https://www.niaaa.nih.gov/ncanda-data-distribution-agreement.

REFERENCES

1. Griswold MG, Fullman N, Hawley C, Arian N, Zimsen SRM, Tymeson HD, et al. Alcohol use and burden for 195 countries and territories, 1990–2016: a systematic analysis for the global burden of disease study 2016. Lancet. 2018;392:1015–35. [PubMed: 30146330]
2. American Psychiatric Association (APA). Diagnostic and Statistical Manual of Mental Disorders Washington, DC: American Psychiatric Association Publishing; 2022.
3. Daviet R, Aydogan G, Jagannathan K, Spilka N, Koellinger PD, Kranzler HR, et al. Associations between alcohol consumption and gray and white matter volumes in the UK biobank. Nat Commun. 2022;13:1175. [PubMed: 35246521]
4. Li L, Yu H, Liu Y, Meng Y, Li X, Zhang C, et al. Lower regional grey matter in alcohol use disorders: evidence from a voxel-based meta-analysis. BMC Psychiatry. 2021;21:247. [PubMed: 33975595]
5. Mackey S, Allgaier N, Chaarani B, Spechler P, Orr C, Bunn J, et al. ENIGMA Addiction Working Group. Mega-analysis of gray matter volume in substance dependence: general and substance-specific regional effects. Am J Psychiatry. 2019;176:119–28. [PubMed: 30336705]

6. Morris VL, Owens MM, Syan SK, Petker TD, Sweet LH, Oshri A, et al. Associations between drinking and cortical thickness in younger adult drinkers: findings from the human connectome project. Alcohol Clin Exp Res. 2019;43:1918–27. [PubMed: 31365137]
7. de Goede J, van der Mark-Reeuwijk KG, Braun KP, le Cessie S, Durston S, Engels RCME, et al. Alcohol and brain development in adolescents and young adults: a systematic review of the literature and advisory report of the Health Council of the Netherlands. Adv Nutr. 2021;12:1379–410. [PubMed: 33530096]
8. Infante MA, Eberson SC, Zhang Y, Brumback T, Brown SA, Colrain IM, et al. Adolescent binge drinking is associated with accelerated decline of gray matter volume. Cereb Cortex. 2022;32: 2611–20. [PubMed: 34729592]
9. Pfefferbaum A, Rohlfing T, Pohl KM, Lane B, Chu W, Kwon D, et al. Adolescent development of cortical and white matter structure in the NCANDA sample: role of sex, ethnicity, puberty, and alcohol drinking. Cereb Cortex. 2016;26:4101–21. [PubMed: 26408800]
10. Squeglia LM, Ball TM, Jacobus J, Brumback T, McKenna BS, Nguyen-Louie TT, et al. Neural predictors of initiating alcohol use during adolescence. Am J Psychiatry. 2017;174:172–85. [PubMed: 27539487]
11. Henderson KE, Vaidya JG, Kramer JR, Kuperman S, Langbehn DR, O'Leary DS. Cortical thickness in adolescents with a family history of alcohol use disorder. Alcohol Clin Exp Res. 2018;42: 89–99. [PubMed: 29105114]
12. Spindler C, Trautmann S, Alexander N, Bröning S, Bartscher S, Stuppe M, et al. Meta-analysis of grey matter changes and their behavioral characterization in patients with alcohol use disorder. Sci Rep. 2021;11:5238. [PubMed: 33664372]
13. Ottino-Gonzalez J, Albaugh MD, Cao Z, Cupertino RB, Schwab N, Spechler PA, et al. Brain structural covariance network differences in adults with alcohol dependence and heavy drinking adolescents. Addiction. 2022;117:1312–25. [PubMed: 34907616]
14. Alexander-Bloch A, Giedd JN, Bullmore E. Imaging structural covariance between human brain regions. Nat Rev Neurosci. 2013;14: 322–36. [PubMed: 23531697]
15. Sporns O Network attributes for segregation and integration in the human brain. Curr Opin Neurobiol. 2013;23:162–71. [PubMed: 23294553]
16. Holla B, Panda R, Venkatasubramanian G, Biswal B, Bharath RD, Benegal V. Disrupted resting brain graph measures in individuals at high risk for alcoholism. Psychiatry Res Neuroimaging. 2017;265: 54–64. [PubMed: 28531764]
17. Jiang G, Wen X, Qiu Y, Zhang R, Wang J, Li M, et al. Disrupted topological organization in whole-brain functional networks of heroin-dependent individuals: a resting-state fMRI study. PLOS ONE. 2013; 8:e82715. [PubMed: 24358220]
18. Sjoerds Z, Stufflebeam SM, Veltman DJ, van den Brink W, Penninx BWJH, Douw L. Loss of brain graph network efficiency in alcohol dependence. Addict Biol. 2017;22:523–34. [PubMed: 26692359]
19. Wang Z, Suh J, Li Z, Li Y, Franklin T, O'Brien C. A hyper-connected but less efficient small-world network in the substance-dependent brain. Drug Alcohol Depend. 2015;152:102–8. [PubMed: 25957794]
20. Zhai J, Luo L, Qiu L, Kang Y, Liu B, Yu D, et al. The topological organization of white matter network in internet gaming disorder individuals. Brain Imaging Behav. 2017;11:1769–78. [PubMed: 27815774]
21. Vijayakumar N, Ball G, Seal ML, Mundy L, Whittle S, Silk T. The development of structural covariance networks during the transition from childhood to adolescence. Sci Rep. 2021;11:9451. [PubMed: 33947919]
22. Albaugh MD, Nguyen TV, Ducharme S, Collins DL, Botteron KN, D'Alberto N, et al. Brain Development Cooperative Group. Age-related volumetric change of limbic structures and subclinical anxious/depressed symptomatology in typically developing children and adolescents. Biol Psychol. 2017;124:133–40. [PubMed: 28185945]
23. Bava S, Tapert SF. Adolescent brain development and the risk for alcohol and other drug problems. Neuropsychol Rev. 2010;20:398–413. [PubMed: 20953990]

24. Dayan J, Bernard A, Olliac B, Mailhes AS, Kermarrec S. Adolescent brain development, risk-taking and vulnerability to addiction. J Pysiol Paris. 2010;104:279–86.
25. Ducharme S, Hudziak JJ, Botteron KN, Albaugh MD, Nguyen TV, Karama S, et al. Decreased regional cortical thickness and thinning rate are associated with inattention symptoms in healthy children. J Am Acad Child Adolesc Psychiatry. 2012;51:18–27.e2. [PubMed: 22176936]
26. Geier CF. Adolescent cognitive control and reward processing: implications for risk taking and substance use. Horm Behav. 2013;64: 333–42. [PubMed: 23998676]
27. Albaugh MD, Ducharme S, Karama S, Watts R, Lewis JD, Orr C, et al. Brain Development Cooperative Group. Anxious/depressed symptoms are related to microstructural maturation of white matter in typically developing youths. Dev Psychopathol. 2017;29:751–8. [PubMed: 27297294]
28. Jernigan TL, Brown TT, Hagler DJ Jr, Akshoomoff N, Bartsch H, Newman E, et al. Pediatric Imaging, Neurocognition and Genetics Study. The pediatric imaging, neurocognition, and genetics (PING) data repository. Neuroimage. 2016;124:1149–54. [PubMed: 25937488]
29. Brown SA, Brumback T, Tomlinson K, Cummins K, Thompson WK, Nagel BJ, et al. National Consortium on alcohol and NeuroDevelopment in adolescence (NCANDA). A multisite study of adolescent development and substance use. J Stud Alcohol Drugs. 2015;76: 895–908. [PubMed: 26562597]
30. Pfefferbaum A, Zahr NM, Sassoon SA, Kwon D, Pohl KM, Sullivan EV. Accelerated and premature aging characterizing regional cortical volume loss in human immunodeficiency virus infection: contributions from alcohol, substance use, and hepatitis C coinfection. Biol Psychiatry Cogn Neurosci Neuroimaging. 2018;3: 844–59. [PubMed: 30093343]
31. Phillips RD, de Bellis MD, Brumback T, Clausen AN, Clarke-Rubright EK, Haswell CC, et al. Volumetric trajectories of hippocampal subfields and amygdala nuclei influenced by adolescent alcohol use and lifetime trauma. Transl Psychiatry. 2021;11:154. [PubMed: 33654086]
32. Squeglia LM, Spadoni AD, Infante MA, Myers MG, Tapert SF. Initiating moderate to heavy alcohol use predicts changes in neuropsycho-logical functioning for adolescent girls and boys. Psychol Addict Behav. 2009;23:715–22. [PubMed: 20025379]
33. Sullivan E, Brumback T, Tapert SF, Brown SA, Baker FC, Colrain IM, et al. Disturbed cerebellar growth trajectories in adolescents who initiate alcohol drinking. Biol Psychiatry. 2020;87:632–44. [PubMed: 31653477]
34. Zhao Q, Sullivan E, Honnorat N, Adeli E, Podhajsky S, de Bellis MD, et al. Association of heavy drinking with deviant fiber tract development in frontal brain systems in adolescents. JAMA Psychiatry. 2021;78:407–15. [PubMed: 33377940]
35. van Essen DC, Smith SM, Barch DM, Behrens TEJ, Yacoub E, Ugurbil K. The WU-Minn human connectome project: an overview. Neuroimage. 2013;80:62–79. [PubMed: 23684880]
36. Fischl B FreeSurfer. Neuroimage. 2012;62:774–81. [PubMed: 22248573]
37. Desikan RS, Ségonne F, Fischl B, Quinn BT, Dickerson BC, Blacker D, et al. An automated labeling system for subdividing the human cerebral cortex on MRI scans into gyral based regions of interest. Neuroimage. 2006;31:968–80. [PubMed: 16530430]
38. Glasser MF, Smith SM, Marcus DS, Andersson JLR, Auerbach EJ, Behrens TEJ, et al. The human connectome project's neuroimaging approach. Nat Neurosci. 2016;19:1175–87. [PubMed: 27571196]
39. Fortin J-P, Cullen N, Sheline YI, Taylor WD, Aselcioglu I, Cook PA, et al. Harmonization of cortical thickness measurements across scanners and sites. Neuroimage. 2018;167:104–20. [PubMed: 29155184]
40. van Wijk BCM, Stam CJ, Daffertshofer A. Comparing brain networks of different size and connectivity density using graph theory. PLOS ONE. 2010;5:e13701. [PubMed: 21060892]
41. Power JD, Schlaggar BL, Lessov-Schlaggar CN, Petersen SE. Evidence for hubs in human functional brain networks. Neuron. 2013; 79:798–813. [PubMed: 23972601]
42. Watson CG, Stopp C, Newburger JW, Rivkin MJ. Graph theory analysis of cortical thickness networks in adolescents with d-transposition of the great arteries. Brain Behav. 2018;8(2):e00834. 10.1002/brb3.834 [PubMed: 29484251]

43. Ho DE, King G, Stuart EA, Imai K. MatchIt: nonparametric preprocessing for. J Stat Softw. 2011;42:1–28.
44. Benjamini Y, Hochberg Y. Controlling the false discovery rate: a practical and powerful approach to multiple testing. J R Stat Soc B Methodol. 1995;57:289–300.
45. R Core Team. R: A Language and Environment for Statistical Computing. Vienna, Austria: R Core team; 2018. Available at: https://www.r-project.org/
46. Alexander-Bloch A, Shou H, Liu S, Satterthwaite TD, Glahn DC, Shinohara RT, et al. On testing for spatial correspondence between maps of human brain structure and function. Neuroimage. 2018;178: 540–51. [PubMed: 29860082]
47. Angebrandt A, Abulseoud OA, Kisner M, Diazgranados N, Momenan R, Yang Y, et al. Dose-dependent relationship between social drinking and brain aging. Neurobiol Aging. 2022;111: 71–81. [PubMed: 34973470]
48. Liao X, Vasilakos A, He Y. Small-world human brain networks: perspectives and challenges. Neurosci Biobehav Rev. 2017;77: 286–300. [PubMed: 28389343]
49. Wang R, Liu M, Cheng X, Wu Y, Hildebrandt A, Zhou C. Segregation, integration, and balance of large-scale resting brain networks configure different cognitive abilities. Proc Natl Acad Sci. 2021; 118:23.
50. Zhang Y, Wang Y, Chen N, Guo M, Wang X, Chen G, et al. Age-associated differences of modules and hubs in brain functional networks. Front Aging Neurosci. 2021;12:607445. [PubMed: 33536893]
51. Gozdas E, Holland SK, Altaye M. Developmental changes in functional brain networks from birth through adolescence. Hum Brain Mapp. 2019;40:434–1444.
52. Baum GL, Ciric R, Roalf DR, Betzel RF, Moore TM, Shinohara RT, et al. Modular segregation of structural brain networks supports the development of executive function in youth. Curr Biol. 2017;27: 1561–1572.e8. [PubMed: 28552358]
53. Shnitko TA, Liu Z, Wang X, Grant KA, Kroenke CD. Chronic alcohol drinking slows brain development in adolescent and young adult nonhuman primates. eNeuro. 2019;6:0044–19.2019.
54. Toga AW, Thompson PM, Sowell ER. Mapping brain maturation. Trends Neurosci. 2006;29:148–59. [PubMed: 16472876]
55. Brion M, D'Hondt F, Pitel A-L, Lecomte B, Ferauge M, de Timary P, et al. Executive functions in alcohol-dependence: a theoretically grounded and integrative exploration. Drug Alcohol Depend. 2017; 177:39–47. [PubMed: 28554151]
56. Powell A, Sumnall H, Kullu C, Owens L, Montgomery C. Subjective executive function deficits in hazardous alcohol drinkers. J Psychopharmacol. 2021;35:1375–85. [PubMed: 34278885]
57. Ducharme S, Albaugh MD, Nguyen T-V, Hudziak JJ, Mateos-Pérez JM, Labbe A, et al. Trajectories of cortical thickness maturation in normal brain development—the importance of quality control procedures. Neuroimage. 2016;125:267–79. [PubMed: 26463175]
58. Kim H-J, Shin J-H, Han CE, Kim HJ, Na DL, Seo SW, et al. Using individualized brain network for analyzing structural covariance of the cerebral cortex in Alzheimer's patients. Front Neurosci. 2016;10:394. [PubMed: 27635121]
59. Sha Z, van Rooij D, Anagnostou E, Arango C, Auzias G, Behrmann M, et al. Subtly altered topological asymmetry of brain structural covariance networks in autism spectrum disorder across 43 datasets from the ENIGMA consortium. Mol Psychiatry. 2022;27:2114–25. [PubMed: 35136228]
60. Bayer JMM, Thompson PM, Ching CRK, Liu M, Chen A, Panzenhagen AC, et al. Site effects how-to and when: an overview of retrospective techniques to accommodate site effects in multi-site neuroimaging analyses. Front Neurol. 2022;13:923988. [PubMed: 36388214]
61. Pomponio R, Erus G, Habes M, Doshi J, Srinivasan D, Mamourian E, et al. Harmonization of large MRI datasets for the analysis of brain imaging patterns throughout the lifespan. Neuroimage. 2020;208: 116450. [PubMed: 31821869]
62. Chen AA, Beer JC, Tustison NJ, Cook PA, Shinohara RT, Shou H. Mitigating site effects in covariance for machine learning in neuroimaging data. Hum Brain Mapp. 2022;43:1179–95. [PubMed: 34904312]

63. Beer JC, Tustison NJ, Cook PA, Davatzikos C, Sheline YI, Shinohara RT, et al. Longitudinal ComBat: a method for harmonizing longitudinal multi-scanner imaging data. Neuroimage. 2020;220: 117129. [PubMed: 32640273]

64. Pohl KM, Sullivan EV, Podhajsky S, Baker FC, Brown SA, Duncan B, et al. The NCANDA_PUBLIC_4Y_REDCAP_V02 Data Release of the National Consortium on Alcohol and NeuroDevelopment in Adolescence (NCANDA). Sage Bionetworks Synapse. 2023. Available at:10.7303/syn24226662 (accessed July 2022).

65. Pohl KM, Sullivan EV, Pfefferbaum A. The NCANDA_PUBLIC_4Y_-STRUCTURAL_V01 Data Release of the National Consortium on Alcohol and NeuroDevelopment in Adolescence (NCANDA). Sage Bionetworks Synapse. Available at: 10.7303/syn22216457 (accessed July 2022).

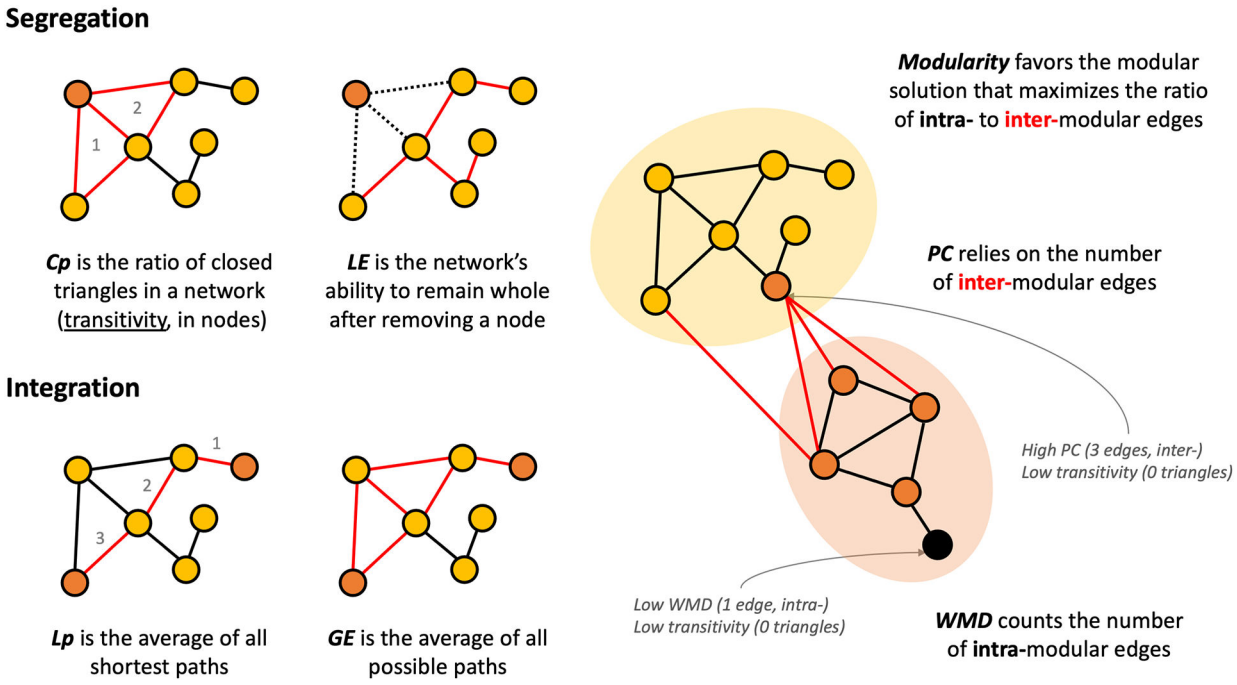

FIGURE 1.

Visual summary of graph theory metrics of segregation, integration and modularity.

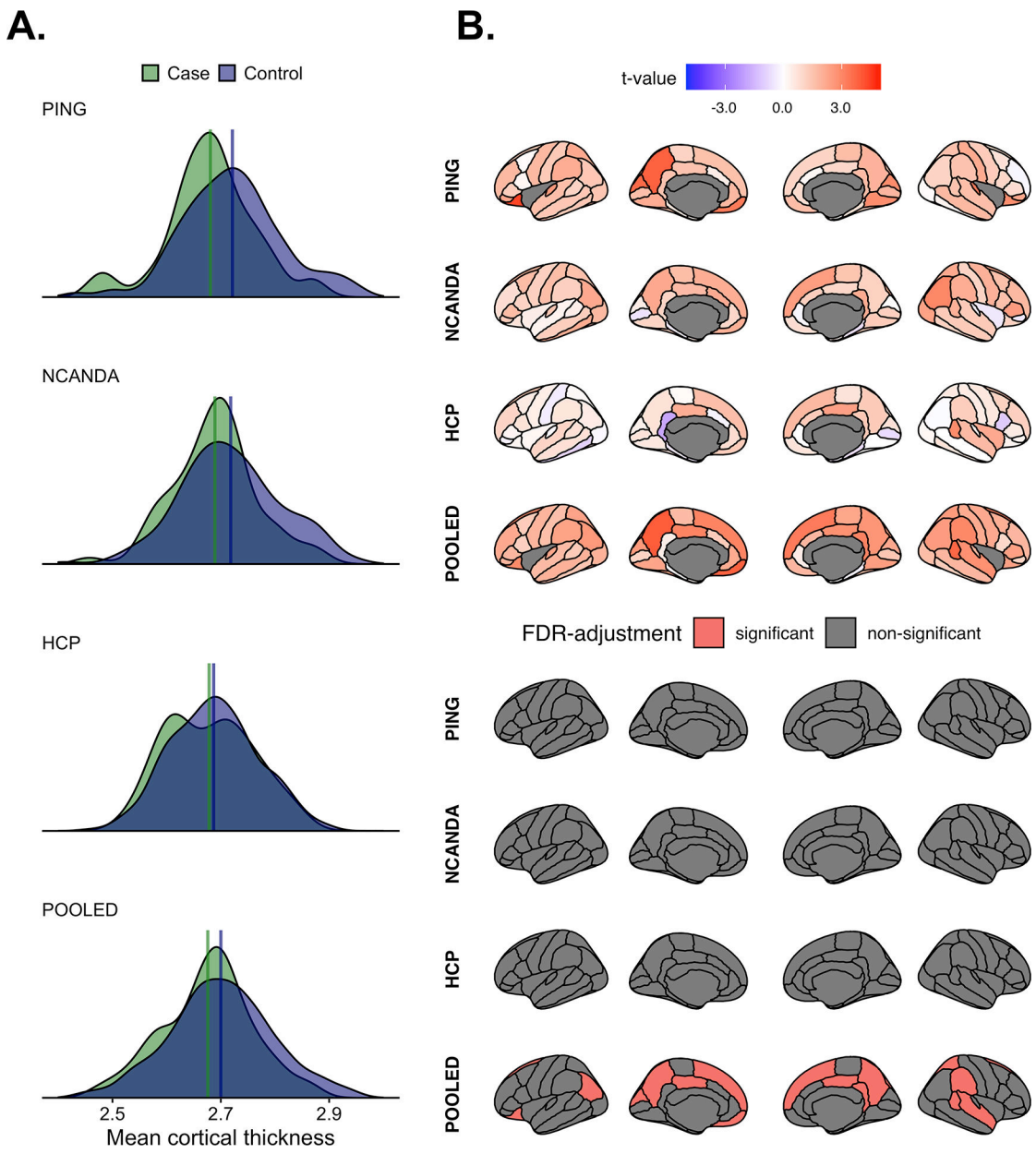

FIGURE 2.

(a) The distributions of mean cortical thickness per group and study. The upper portion of (b) shows the between-group differences in regional cortical thickness. Positive *t*-values indicate greater thickness in controls. Bottom portion of (b) shows regions surviving study-wise false discovery rate (FDR)-correction.

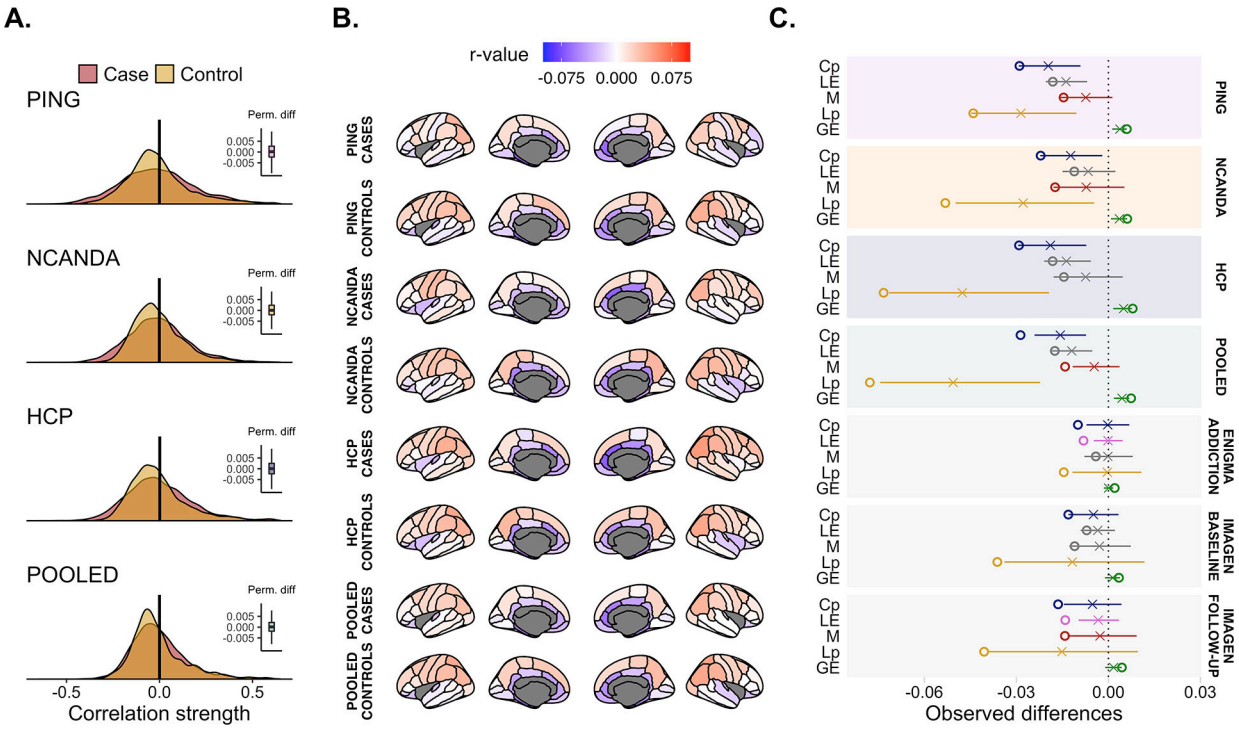

FIGURE 3.

(a) Overlap in the global correlation strength between groups. The vertical black line indicates the observed difference and the right-sided box-plot the permuted difference. No significant group differences were observed. (b) The average correlation strength per region-of-interest (ROI) and shows the similarity in regional correlation weights across both groups and studies. (c) Summary of the network-level metrics of the current study together with the summary statistics of our previous work. The horizontal line denotes the null distribution, the X the mean permuted difference under the null hypothesis and the circle the observed difference. If colored, the area under the curve (AUC) difference was significant ($P < 0.05$), otherwise the data are presented in grey. Cp = clustering coefficient; LE = local efficiency; M = modularity; Lp = average shortest path length; GE = global efficiency.

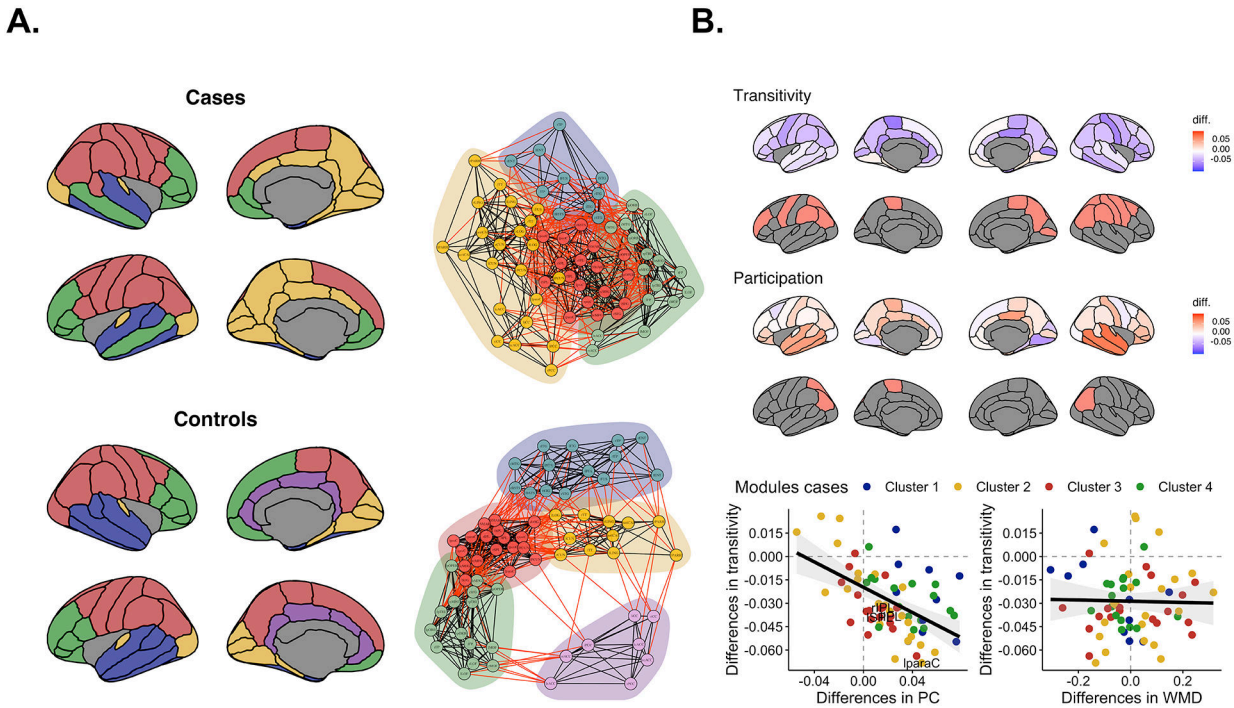

FIGURE 4.

(a) The different modules for cases and controls at their maximum density (30%). Red edges indicate intermodular correlations and black edges intramodular correlations. Greater overlap of modules represents more intermodule thickness similarities. (b) The upper row shows the unthresholded differences in transitivity and the second row shows nodes passing statistically significant cut-offs ($P < 0.05$). Blue indicates lower transitivity in cases. The middle row shows the unthresholded differences in the participation coefficient and below it the nodes passing cut-offs for statistical significance ($P < 0.05$). Red represents higher participation coefficient (PC) in cases. Bottom row depicts the correlation between the unthresholded differences in transitivity, PC and within-modular degree (WMD). Points are colored based on the modular organization of cases.

Table 1 –

Summary of demographics per group and study.

Dataset	Group	N	Age (mean, sd)	Age range	Females	stats	sig
PING	Cases	50	18.1 ± 1.97	14 – 21	26 (52%)	t = 0.85 X^2 = *0*	p = 0.40 p=l
	Controls	350	17.8 ± 2.03	14 – 21	182 (52%)		
NCANDA	Cases	68	19.53 ± 0.99	17.5 – 21.6	30 (44.1%)	t = 1.53 X^2 = 0	p = 0.13 p = 0.78
	Controls	204	19.32 ± 0.97	17.4 – 21.9	96 (47.1%)		
HCP	Cases	61	28.8 ± 3.33	23 – 36	34 (55.7%)	t = −0.20 X^2 = 0.14	p = 0.84 p = 0.71
	Controls	314	28.9 ± 3.84	22 – 37	186 (59.2%)		
POOLED	Cases	179	22.3 ± 5.26	14 – 36	90 (50%)	t = 0.24 X^2 = 0.48	p = 0.81 p = 0.49
	Controls	868	22.2 ± 5.77	14 – 37	464 (53.5%)		

Note: *t*-student is for age (continuous) and X^2 for sex (categorical) comparisons